Piezoelectric-Driven Self-Sensing Leaf-Mimic Actuator Enabled by Integration of a Self-Healing Dielectric Elastomer and a Piezoelectric Composite

Min Pan, Chenggang Yuan, Tom Pickford, Jianhui Tian, Christopher Ellingford, Ning Zhou, Christopher Bowen, and Chaoying Wan*

Soft robots and devices exploit highly deformable materials that are capable of changes in shape to allow conformable physical contact for controlled manipulation. While soft robots are resilient to mechanical impact, they are susceptible to mechanical damage, such as tears and punctures. The development of self-healing materials and actuators continues to attract increasing interest, in particular, with respect to integrating self-healing polymers to create bioinspired soft self-healing devices. Herein, a novel piezoelectric-driven self-healing leaf-motion mimic actuator is designed by combining a thermoplastic methyl thioglycolate–modified styrene–butadiene–styrene (MGSBS) elastomer with a piezoelectric macrofiber composite (MFC) for self-sensing applications. This article is the first demonstration of a self-sensing and self-healing actuator-sensor system, which is driven by a piezoelectric actuator and can mimic leaf motion. The leaf-motion actuator combines built-in dynamic sensing and room-temperature self-healing capabilities to restore macroscale cutting damage with an intrinsically high bandwidth of up to 10 kHz. The feasibility and potential of the new actuator for use in complex soft autonomous systems are demonstrated. These new results help to address the emerging influence of self-healing soft actuators and the challenges of sensing, actuation, and damage resistance in soft robotics.

Self-healing dielectric elastomers are promising for bioinspired actuator and generator applications due to their unique characteristics, such as their lightweight nature, low cost, ease of processing, extended durability, and operational reliability.[1] For example, dielectric elastomer actuators are required to undergo cyclic mechanical deformation when subjected to high electric fields;[2] therefore, they need both high mechanical elasticity and high dielectric permittivity to ensure a high efficiency. In addition, self-healable dielectric elastomers are promising materials for the design of high-performance muscle-like actuators.[3]

Due to the low Young's modulus, silicone-based elastomers have been widely investigated for actuators and soft systems[4] capable of providing a smooth expansion and contraction at high levels of strain. Recent advances in self-healing technologies have provided a route to create more durable silicone-based soft devices.[5] Bao et al. reported a self-healing polydimethylsiloxane that was crosslinked by coordination complexes to provide high strain, high dielectric strength, and large actuation levels.[6] The materials expanded by 3.6% under a high applied electric potential of 11 kV when used for artificial muscle

Dr. M. Pan, C. Yuan, Dr. J. Tian, Dr. N. Zhou, Prof. C. Bowen
Department of Mechanical Engineering
University of Bath
BA2 7AY Bath, UK

T. Pickford, C. Ellingford, Dr. C. Wan
International Institute for Nanocomposites Manufacturing (IINM)
WMG
University of Warwick
CV4 7AL Coventry, UK
E-mail: chaoying.wan@warwick.ac.uk

(iD) The ORCID identification number(s) for the author(s) of this article can be found under https://doi.org/10.1002/aisy.202000248.

Dr. J. Tian
CAE Analysis Room for Engineering Applications
School of Mechatronic Engineering
Xi'an Technological University
Xi'an 710021, China

Dr. N. Zhou
Key Laboratory of Education Ministry for Modern Design and Rotor-Bearing System
School of Mechanical Engineering
Xi'an Jiaotong University
Xi'an 710049, China

**ADVANCED
SCIENCE NEWS**

www.advancedsciencenews.com

**ADVANCED
INTELLIGENT
SYSTEMS**
Open Access

www.advintellsyst.com

applications. After experiencing dielectric breakdown at 12 kV, the elastomeric muscle was able to heal rapidly and recover its mechanical properties. By combining electrical and hydraulic fluid-driven mechanisms, Keplinger and co-workers[7] designed a hydraulically amplified self-healing electrostatic (HASEL) actuator from innovative liquid dielectrics and demonstrated their muscle-like deformation and self-healing ability after repeated dielectric breakdown events. Starting at an initial breakdown voltage of 29 kV, an average breakdown voltage of 23.8 kV was obtained over 50 cycles of breakdown and recovery. The HASEL device was successfully actuated using an applied voltage of 12 kV at a frequency of 50 Hz, demonstrating a controllable linear contraction of up to 10%, a strain rate of 900% per second, and the ability to lift over 200 times its weight.[1b] These properties provide this device with a great potential for use in applications, such as active prostheses, medical and industrial automation, and autonomous robotic devices.

Terryn et al. reported on a soft self-healing pneumatic actuator formed using Diels–Alder chemistry.[8] Two damage conditions were considered: 1) the formation of a small perforation through the application of a high pressure and 2) a deep wall cut, with a length of 4.43 mm and a thickness of 0.3 mm. Both types of mechanical damage were successfully healed, with a maximum temperature treatment of 70 °C after 30 h. They demonstrated self-healing applications using the developed self-healing polymers, including a soft gripper, a soft hand, and artificial muscles. The devices self-healed after a heat treatment of 80 °C for 40 min, followed by slow cooling to 25 °C. After a period of 24 h at 25 °C, the initial properties were almost entirely recovered.[9] We recently developed a facile and scalable approach to successfully convert a commodity thermoplastic elastomer, styrene–butadiene–styrene (SBS), into a self-healing dielectric elastomer.[10] Using a one-step click chemistry method, a range of organic polar groups, such as methyl thioglycolate,[10b] methyl-3-mercaptopropionate,[11] and/or thioglycolic acid,[12] can be chemically grafted to the elastomer backbone through thiol-ene reactions. The structure and graft ratios of the polar groups can be used to tailor the polarity, relative permittivity, and mechanical extensibility of the elastomers. In addition, the introduction of polar groups simultaneously enhances the intra- and inter-macromolecular interactions and, thus, enables a self-healing function. The intrinsic modification of dielectric elastomers shows unprecedented advantages over conventional blending or composting methods and represents a promising approach for large scale applications in soft robotics, medical devices, artificial muscles, and energy-harvesting systems.

Here, we use a methyl thioglycolate–modified SBS (MGSBS) elastomer as a self-healing material to create a leaf-mimic actuator. The synthesis, structural characterization, and electrical and mechanical properties before and after self-healing have been investigated in detail in our previous work.[10] The MGSBS elastomer has an MG grafting ratio of 98.3% and exhibits a high strain ($\approx$569%), high relative permittivity ($\varepsilon_r \approx 12$), and a high self-healing efficiency of 25.4% of tensile strength at room temperature. The MGSBS-based actuator could recover its dielectric strength by 79% after dielectric breakdown at an applied potential of 9.25 kV. More importantly, the high relative permittivity of MGSBS typically exceeds that of silicone elastomers ($\varepsilon_r \approx 2$–10). Similarly, Young's modulus (2.87 MPa), strain at break (569%),

and tensile strength of MGSBS (3.13 MPa) are significantly higher than chemically crosslinked silicone elastomers.[4] The higher strain at break of MGSBS, combined with its intrinsic self-healing function, makes it highly appealing for high electric field applications.

To date, there has been limited work on the dynamics of soft self-healing devices subjected to mechanical damage.[13] In this work, inspired by the waving motion of natural leaves, we integrated a piezoelectric actuator, sensor, and self-healing elastomer (MGSBS) and developed a high bandwidth, self-sensing, and self-healing biomimetic leaf actuator. The actuation behavior and the effect of mechanical damage on the leaf actuator dynamics are investigated using a power spectrum and time-frequency analysis[14] of experimental data and finite-element models (FEMs) to demonstrate the potential of using self-healing polymers for the development of dynamic soft actuators.

The synthesis and structural characterization of MGSBS and evaluation of its dielectric actuator applications have been discussed in detail in our previous research.[10] To understand the performance of the combination of a self-healing elastomer with a piezoelectric composite actuator, we will investigate the effectiveness of self-healing MGSBS as a leaf-like actuator.

A 3D-printed leaf shape template was manufactured and used to fabricate self-healing leaves to ensure shape consistency. MGSBS was manufactured by grafting a polar methyl thioglycolate group on the polymer backbone of an SBS elastomer. The synthesis is a one-step thiol-ene click reaction at room temperature, and the experimental details are provided in the Experimental Section. The obtained MGSBS was compression molded at 180 °C to form MGSBS elastomer sheets, which were subsequently shaped using the leaf-geometry template. The self-healing leaf had a width of 42 mm and a length of 70 mm. The leaf tip angle was 40°, as shown in **Figure 1**a. To provide both actuation and strain sensing functions, two piezoelectric macro-fiber composites (MFCs) were bonded to the MGSBS leaf using a silicone adhesive (Smooth-On, Sil-Poxy) and cured for a period of 36 h. NASA's MFC was invented in 1999 and is one of the leading low-profile actuators and sensors offering high strain performance, mechanical flexibility, and reliability in cost-efficient applications. An MFC M4005-P1 was used to drive the MGSBS leaf to induce movement, whereas a second MFC was used to measure leaf movement using it as a sensitive piezoelectric strain sensor. A summary of the MFC properties can be found in the previous study.[15] The fabricated piezoelectric-driven self-healing leaf prototype is shown in Figure 1b.

A high-power amplifier E-481 from Physik Instrumente was used to supply a high driving voltage to actuate the MFC, where the operating range was −500 to +1500 V. The experimental setup is shown in Figure 1c, and video, Supporting Information. To evaluate how the self-healing would benefit the operation of the soft devices, we designed a setup to test the dynamic response of the original, cut, and healed leaf, as shown in Figure 1d. The leaf tip (18 mm in length) was initially cut, and then left at room temperature for 24 h to heal. The dynamic responses of the 1) original; 2) broken; and 3) healed leaves were characterized. During dynamic testing, the piezoelectric-driven self-healing leaf was driven using a sinusoidal voltage signal that was swept across the frequency range of 1–50 Hz, with a step frequency of 2 Hz. The amplitude
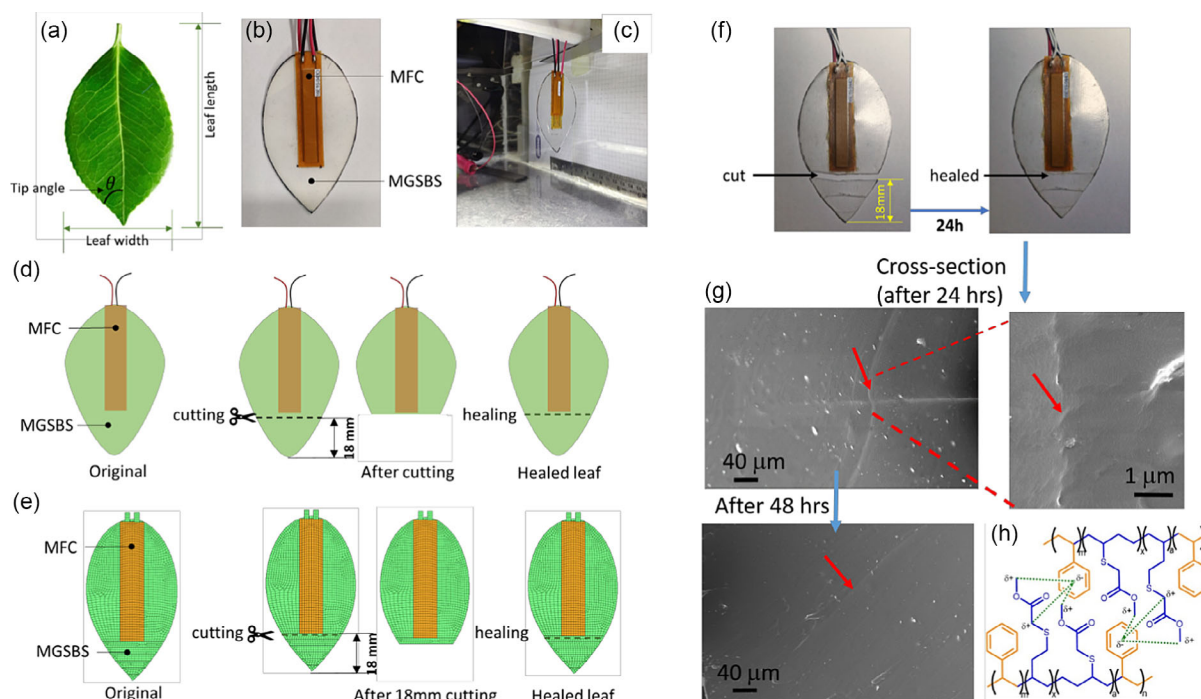
**ADVANCED
SCIENCE NEWS**

www.advancedsciencenews.com

**ADVANCED
INTELLIGENT
SYSTEMS**
Open Access

www.advintellsyst.com

Figure 1. a) Bioinspired self-healing leaf concept. b) Photograph of piezoelectric-driven self-healing leaf prototype. c) Experimental setup. d) Original, cut (damaged), and healing states of the leaf. e) Simulated leaf in original, broken, and healed states in ANSYS. f) Experimental leaf in original, broken, and healed states. g) Scanning electron microscopy observation of the cross section of the healed MGSBS sheet; the sheet was cut through as shown in (f) followed by placing the two pieces back into contact and leaving for 24 h at room temperature to heal. h) Self-healing mechanism of MGSBS via the interchain electrostatic interactions.

of the driven actuator signal was 500 V. After this initial testing, the leaf tip was cut and removed, and the "broken" leaf was tested driven by the same input voltage. After pressing the leaf tip and "broken" piece together and leaving for 24 h, the leaf was completely healed. To understand the impact of the degree of damage on the leaf dynamics, an FEM of the leaf with different degrees of damage/cuts, up to 18 mm, was developed, as shown in Figure 1e, with the experimental equivalent shown in Figure 1f.

Figure 1g shows a cross section of the healed MGSBS sheets after 24 and 48 h of healing, which indicates that the cut line is merged and healed after 24 h, and is nearly invisible after 48 h.

The self-healing behavior of MGSBS originates from the $\delta+$ protons adjacent to the ester of methyl thioglycolate that electrostatically interact with the $\delta-$ aromatic center of styrene. This interaction also compatibilizes the normally phase-separated SBS block copolymer morphology, as confirmed in our previous work.[10] In addition to visual inspection of the damage site, the recovery of tensile strength and the strain at break after self-healing of the MGSBS were evaluated by mechanical testing, and the extent of recovery of the mechanical properties with self-healing time is shown in **Figure 2**a. The strain at break and tensile strength recovered by 21% and 25% of the
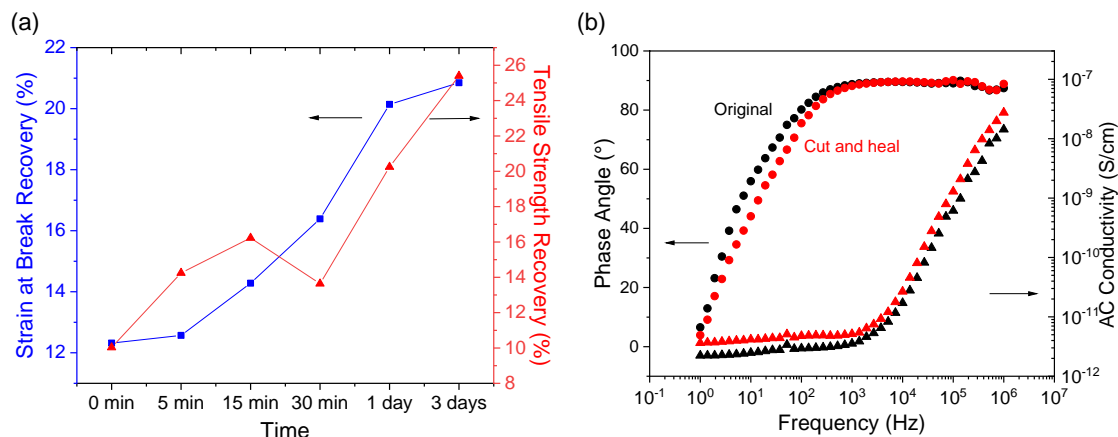

Figure 2. a) Recovery of mechanical properties. b) Phase angle and AC conductivity of MGSBS after self-healing from a slice after various time intervals.

**ADVANCED
SCIENCE NEWS**
www.advancedsciencenews.com

**ADVANCED
INTELLIGENT
SYSTEMS**
Open Access
www.advintellsyst.com

undamaged MGSBS after three days, with potential for greater recovery over a more extended period. An advantage of MGSBS is its room-temperature self-healing ability due to the introduced electrostatic interactions. A higher temperature may weaken the electrostatic interactions, despite the increased mobility of the polymer chains, so that the degree of self-healing recovery reduces. As a result, MGSBS shows the best self-healing performance at room temperature, making the material particularly attractive for thermally sensitive soft systems.

In addition, the dielectric properties of the MGSBS elastomer were examined after self-healing for a period of 24 h. As shown in Figure 2b, the self-healed sample showed complete recovery of electrical properties after a period of 24 h. At low frequencies, the phase angle approaches 0° due to a small degree of conductivity in the MGSBS. This can also be observed as a frequency-independent conductivity of the material (similar to a resistor, R, because conductivity is proportional to R^{-1}). At higher frequencies (100 Hz), the phase approaches 90°, because alternating current (AC) currents are now flowing through the capacitive component of the MGSBS. This can be observed in the stronger frequency dependence of the AC conductivity in the higher frequency range (similar to a capacitor, C, because its AC conductivity is proportional to ωC).
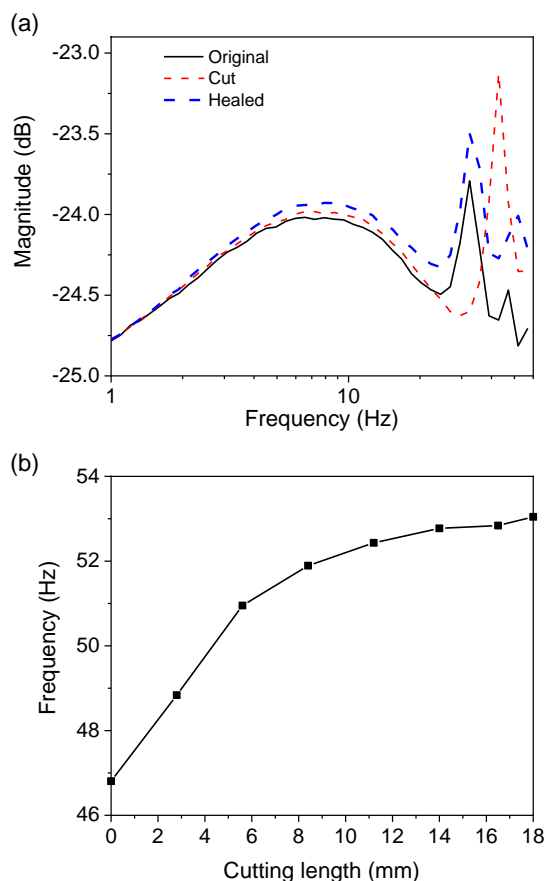

Figure 3. a) Experimental dynamic response of the piezoelectrically driven self-healing leaf. b) The relationship between cutting length and resonance frequencies of different response modes.
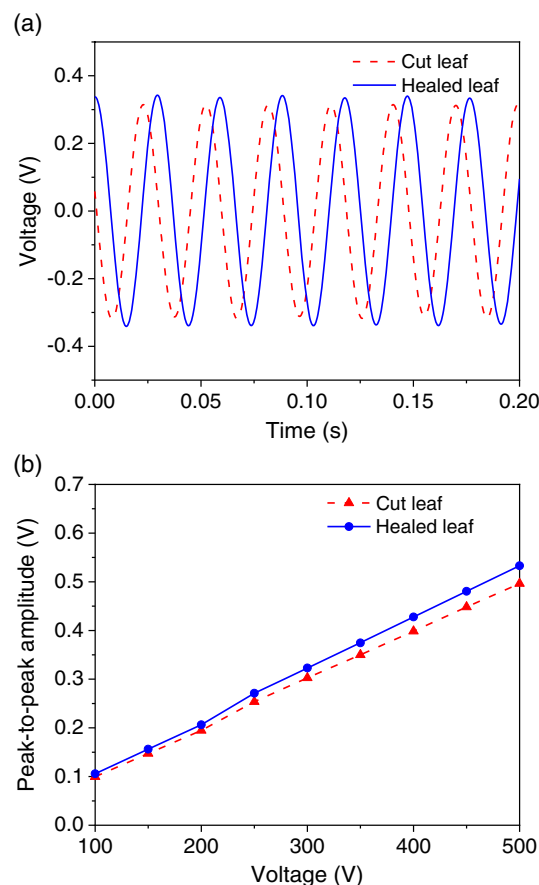

Figure 4. Actuation performance of leaf actuators at different states (cut and healed). a) Time-domain dynamic responses of leaf actuators under a sinusoidal input voltage of 500 V at the excitation frequency of 33 Hz. b) Peak-to-peak amplitudes of waving motion with a range of applied voltage from 100 to 500 V at 33 Hz.

The dynamic responses of the broken (cut) leaf and the self-healed leaf are shown in **Figure 3**a, where the healed leaf has recovered its dynamic response and has a 95% similarity compared with the original leaf. The similarity is defined by analyzing the frequency and amplitude differences between the original and healed leaves in the frequency range of interest (1–50 Hz). The average variation is 4.6%, which led to a similarity of ≈95%. The leaf's resonance frequency has returned to its original value of 33 Hz, where a small amplitude difference of 0.5 dB is observed at this frequency. These results have demonstrated that the dynamics of the device are not impaired by the deflection and leaf healing process. The FEMs were developed using ANSYS Workbench 2019, and further details are presented in the Experimental Section. In the FEM models, we assumed perfect bonding between the healed surfaces, and changes in leaf geometry reflect the introduction of damage, due to cutting, and the subsequent reattachment of the damaged section to the leaf by self-healing. The relationship between the damage (cut) length and the leaf's simulated resonant frequency is shown in Figure 3b, where the resonance frequency increased after cutting due to the smaller dimensions of the leaf actuator. This trend is also observed experimentally, as shown in

Table 1. Properties of MFC and MGSBS.

Item	E_x [MPa]	E_y [MPa]	E_z [MPa]	Mu_{xy}	Mu_{xz}	Mu_{yz}	G_{xy} [GPa]	G_{xy} [GPa]	G_{xy} [GPa]	Density [kg m^{-3}]
MFC	30 000	15 500	15 500	0.35	0.4	0.4	5.7	10.7	10.7	5440
MGSBS	2.87	2.87	2.87	0.3	0.3	0.3	–	–	–	1140

Figure 3a. An approximate 15 Hz difference between the experimental and simulated results is observed for the resonance frequencies of the original (uncut) and broken (cut) leaf. The differences between the simulated and experimental results may be due to the electrical wires coupling with the leaf motion, thereby resulting in complex dynamics that are difficult to model. However, the simulated models correctly predict the dynamic trend in terms of frequency shift with damage and healing, which has been experimentally validated.

Figure 4 shows the actuation performance of the leaf actuator in the broken and healed states. The time-domain dynamic responses of leaf actuators are shown in Figure 4a, where a sinusoidal voltage (±500 V) with a frequency of 33 Hz is used as a drive signal. The broken (cut) leaf exhibited a smaller amplitude and a phase shift of 82° compared with the healed leaf. A phase shift can often impair the dynamic response of a control system, which can lead to system instability. In a stabilized control system, the control object (in this case, the leaf-mimic actuator) is driven by the desired control signal, which is determined by the control algorithm and object dynamics. With the correct and accurate input signal, the leaf should achieve the desired output motion, as required. However, if a phase shift in object dynamics due to damage is not considered during controller design, the phase of the calculated input signal will need to shift to avoid system instability. The healed leaf can effectively eliminate the effect, which provides a promising method of using self-healing materials for manufacturing damage-resistant soft actuators and restoring dynamic properties. Figure 4b shows the peak-to-peak voltage amplitude of two leaves as a function of driving voltage from 100 to 500 V. A linear relationship was achieved for both the broken and healed leaves. The findings can be expanded to create more general and complex soft actuators and provide confidence in using soft self-healing actuators to maneuver in an extreme environment.

This article presents a novel piezoelectric-driven self-healing leaf-mimic actuator that integrates a self-healing MGSBS elastomer with a piezoelectric MFC. The leaf mimic actuator combines the built-in dynamic actuation/sensing of a piezoelectric and the self-healing capabilities of MGSBS to self-heal macroscale damage at room temperature and recover mechanical and dynamic properties, with an intrinsically high bandwidth up to 10 kHz. The work has demonstrated the feasibility and potential of the new actuator to be applied to complex soft autonomous systems and addresses the emerging influence of self-healing soft actuators and the challenges of sensing, dynamic actuation, and damage resistance in soft robotics.

Experimental Section

Synthesis of MGSBS: SBS was purchased from Dexco in pellet form as Vector 8508 A, a linear triblock copolymer. Methyl thioglycolate (95%),
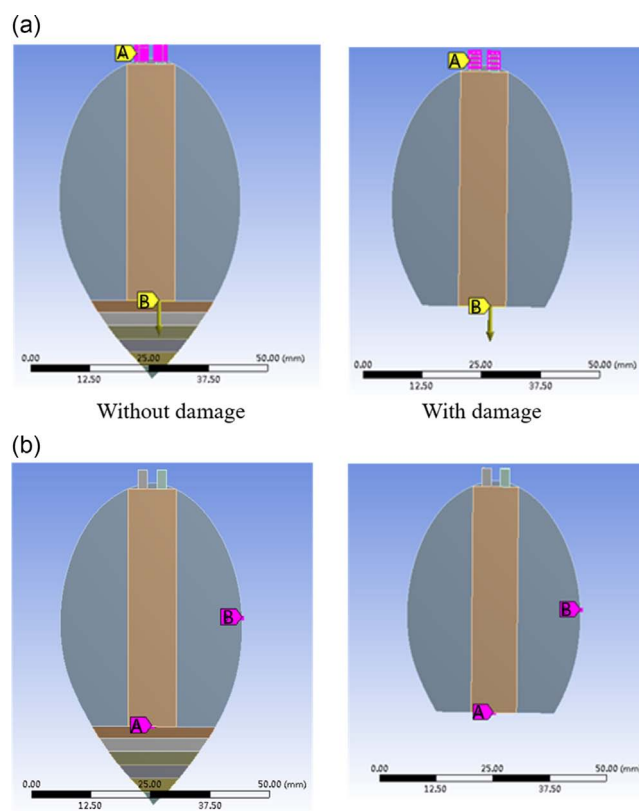

(a)

Without damage   With damage

(b)

Figure 5. a) Ansys model with the boundary condition. b) The A and B observation positions. The frequency of six different modes with different levels of damage can be obtained, as shown in Table S1, Supporting Information. The displacement frequency response from 1 to 80 Hz at observation points A and B is shown in Figure S2, Supporting Information.

2,2-dimethoxy-2-phenylacetophenone (DMPA; 99%), and hexane (HPLC grade, >95%) were purchased from Sigma-Aldrich. Tetrahydrofuran (THF; GPR Rectapur, >99%) was purchased from VWR. MGSBS was synthesized and characterized according to a previously reported method.[10] In short, 10 g of SBS was dissolved in 90 g of THF and 0.2 g of DMPA, and a 4× excess of methyl thioglycolate (46.9 mL) was added into the solution. The solution was irradiated with UV light @ 365 nm under 50 W of power using an OmniCure Series 2000 UV lamp for 20 min. The resulting polymer was concentrated and precipitated three times in hexane and dried for 72 h in a vacuum oven at 40 °C. The final product weight was 21.3 g and had a grafting efficiency of 98.3 mol%.

Tensile testing was performed using a Shimadzu Autograph AGS-X and samples conforming to ASTM-D638-14 type V. The samples were tested at 50 mm min^{-1} with a 10 kN load cell. Healed samples were cut using a scalpel blade, and the surfaces contacted together for a set time period at room temperature before tensile testing and electrical testing. The electrical properties were investigated using impedance spectroscopy via a Princeton Applied Research Parstat MC with a PMC-2000 card and an

in-house two-point probe in the frequency range of 10^0–10^6 Hz, with a film thickness of $\approx 200\ \mu m$.

FEM Modeling: The FEM of the different leaves was built using ANSYS WORKBENCH19.0. A plane stress element was used in the model, where 2975 elements and 3149 nodes were created. The properties of the MFC and MGSBS used in the model are shown in **Table 1**. Fixed boundary conditions were applied to the upper edge of the leaf for modal and harmonic analysis. A 15 μm piezoelectric displacement was applied at the end of the MFC to simulate the displacement at the driving voltage of 500 V, as shown in **Figure 5**a. The resonant frequency of the leaf with different levels of damage is shown in Figure S1, Supporting Information. For the harmonic analysis, the A and B positions are observed for the resonance response, where the observation position can be shown in Figure 5b.

Supporting Information

Supporting Information is available from the Wiley Online Library or from the author.

Conflict of Interest

The authors declare no conflict of interest.

Data Availability Statement

The data that support the findings of this study are available from the corresponding author upon reasonable request.

Keywords

actuation, dielectric elastomers, piezoelectric actuators, self-healing devices, self-sensing applications

[1] a) T. P. Huynh, P. Sonar, H. Haick, *Adv. Mater.* **2017**, *29*, 1604973; b) N. Kellaris, V. G. Venkata, G. M. Smith, S. K. Mitchell, C. Keplinger, *Sci. Robot.* **2018**, *3*, eaar3276.

[2] Y. Zhang, H. Khanbareh, J. Roscow, M. Pan, C. Bowen, C. Wan, *Matter* **2020**, *3*, 989.

[3] M. Y. Benslimane, H. E. Kiil, M. J. Tryson, *Polym. Int.* **2010**, *59*, 415.

[4] a) D. M. Opris, *Adv. Mater.* **2018**, *30*, 1703678; b) E. Perju, Y. S. Ko, S. J. Dünki, D. M. Opris, *Mater. Des.* **2020**, *186*, 108319.

[5] a) L. J. Romasanta, M. A. López-Manchado, R. Verdejo, *Progr. Polym. Sci.* **2015**, *51*, 188; b) D. McCoul, W. Hu, M. Gao, V. Mehta, Q. Pei, *Adv. Electron. Mater.* **2016**, *2*, 1500407.

[6] C.-H. Li, C. Wang, C. Keplinger, J.-L. Zuo, L. Jin, Y. Sun, P. Zheng, Y. Cao, F. Lissel, C. Linder, X. You, Z. Bao, *Nat. Chem.* **2016**, *8*, 618.

[7] E. Acome, S. Mitchell, T. Morrissey, M. Emmett, C. Benjamin, M. King, M. Radakovitz, C. Keplinger, *Science* **2018**, *359*, 61.

[8] a) S. Terryn, G. Mathijssen, J. Brancart, D. Lefeber, G. Van Assche, B. Vanderborght, *Bioinspir. Biomimet.* **2015**, *10*, 046007; b) S. Terryn, J. Brancart, D. Lefeber, G. Van Assche, B. Vanderborght, *Sci. Robot.* **2017**, *2*.

[9] S. Terryn, E. Roels, J. Brancart, G. V. Assche, B. Vanderborght, *Actuators* **2020**, *9*, 34.

[10] a) Y. Zhang, C. Ellingford, R. Zhang, J. Roscow, M. Hopkins, P. Keogh, T. McNally, C. Bowen, C. Wan, *Adv. Funct. Mater.* **2019**, *29*, 1808431; b) C. Ellingford, R. Zhang, A. M. Wemyss, C. Bowen, T. McNally, Ł. Figiel, C. Wan, *ACS Appl. Mater. Interfaces* **2018**, *10*, 38438.

[11] C. Ellingford, R. Zhang, A. M. Wemyss, Y. Zhang, O. B. Brown, H. Zhou, P. Keogh, C. Bowen, C. Wan, *ACS Appl. Mater. Interfaces* **2020**, *12*, 7595.

[12] C. Ellingford, A. M. Wemyss, R. Zhang, I. Prokes, T. Pickford, C. Bowen, V. A. Coveney, C. Wan, *J. Mater. Chem. C* **2020**, *8*, 5426.

[13] M. D. Bartlett, M. D. Dickey, C. Majidi, *NPG Asia Mater.* **2019**, *11*, 21.

[14] a) G.-R. Gillich, Z.-I. Praisach, *Signal Process.* **2014**, *96*, 29; b) U. Lee, J. Shin, *Comput. Struct.* **2002**, *80*, 117.

[15] Smart Materials, https://www.smart-material.com/MFC-product-properties.html, (accessed: December 2020).